

The Solar Model Problem Solved by the Abundance of Neon in Stars of the Local Cosmos

Jeremy J. Drake¹ & Paola Testa²

¹Harvard-Smithsonian Center for Astrophysics, 60 Garden Street, Cambridge MA 02138, USA.

²MIT Kavli Institute for Astrophysics and Space Research, Massachusetts Institute for Technology, 70 Vassar Street, Cambridge, MA 02139, USA.

The interior structure of the Sun can be studied with great accuracy using observations of its oscillations, similar to seismology of the Earth. Precise agreement between helioseismological measurements and predictions of theoretical solar models¹ has been a triumph of modern astrophysics. However, a recent downward revision by 25-35% of the solar abundances of light elements such as C, N, O and Ne² has broken this accord: models adopting the new abundances incorrectly predict the depth of the convection zone, the depth profiles of sound speed and density, and the helium abundance.^{1,3} The discrepancies are far beyond the uncertainties in either the data or the model predictions.⁴ Here we report on neon abundances relative to oxygen measured in a sample of nearby solar-like stars from their X-ray spectra. They are all very similar and substantially larger than the recently revised solar value. The neon abundance in the Sun is quite poorly determined. If the Ne/O abundance in these stars is adopted for the Sun the models are brought back into agreement with helioseismology measurements.^{5,6}

The role of the Sun as a fundamental benchmark of stellar evolution theory, which itself underpins much of astrophysics, renders the “solar model problem” one of some importance. The schism between helioseismology and models with a revised composition has arisen because abundant elements such as C, N, O and Ne provide major contributions to the opacity of the solar interior, which in turn influences internal structure and the depth at which the interior becomes convective. Uncertainties in the calculated opacities themselves appear insufficient to bridge the gap,^{5,7} and the propriety of the recent abundance revisions has therefore been questioned.

The revised abundances are demanded by new analyses of the visible solar spectrum that take into account convection and associated velocity fields and temperature inhomogeneities through 3-D hydrodynamic modelling, and that relax the assumption of local thermodynamic equilibrium for computing atomic level populations.⁸ The solar abundances of C, N and O can be measured accurately based on their absorption lines. However, Ne lacks detectable photospheric lines in cool stars like the Sun, and the Ne abundance is therefore much less certain. The solar Ne content is assessed based on observations of neon ions in nebular and hot star spectra, and on measurements of solar energetic particles.^{2,9} Measurements are generally made relative to a reference element such as O; the downward revision of the solar O abundance therefore required a commensurate lowering of the Ne abundance for consistency.² Expressed as the ratio of the number of Ne atoms in the gas to those of O, this abundance is $A_{Ne}/A_O = 0.15$, which is very similar to values adopted in earlier studies.^{10,11} However, it has recently been pointed out that the solar model problem could be solved were the true solar Ne abundance to be at least a factor of 2.5 times higher than recently assessed.^{4,5}

We are motivated by the solar model problem to investigate Ne abundances in nearby stars. While not detected in the optical spectra of cool stars, emission lines of highly ionised Ne are prominent features of their X-ray spectra.¹² The Ne/O abundance ratio can be derived directly from the ratio of observed fluxes of the hydrogen-like and helium-like ions of O and Ne (see Methods for details); we adopt a slightly refined version of the method applied to the analysis of earlier solar X-ray spectra.¹³ In this way, we have obtained the Ne/O abundance ratios for a sample of 21 stars lying within 100pc of the Sun that have been observed by the *Chandra* X-ray Observatory using the High Energy Transmission Grating Spectrometer.¹⁴ A representative X-ray spectrum, that of the M1 V star AU Mic, is presented in Figure 1. The stars studied, together with observed Ne and O line fluxes and derived Ne/O abundance ratios are listed in Table 1. The Ne/O abundance ratios are illustrated as a function of the ratio of logarithmic X-ray and bolometric luminosities, L_X/L_{bol} —a commonly used index of stellar coronal activity—in Figure 2. Since our star sample contains more objects toward higher L_X/L_{bol} , we have added Ne/O ratios for two stars of somewhat lower activity level (Procyon, an F5 subgiant, and ϵ Eri, a K2 dwarf) from the literature.¹⁵ There is no trend in

the Ne/O abundance ratio with L_X/L_{bol} , and the error-weighted mean ratio is $A_{Ne}/A_O = 0.41$.

Our derived Ne/O abundance ratio is 2.7 times higher than the currently recommended solar value² but is consistent with the abundance inferred from helioseismology.^{5,6} Solving the solar model problem by raising the Ne abundance alone would require a minimum ratio $A_{Ne}/A_O = 0.52$, or 3.44 times larger than recommended.⁵ However, raising the C, N, O and Fe abundances upward within their estimated uncertainty range of $\pm 12\%$ (adjusting them all together is not unreasonable because the recent downward revisions are correlated) would require an Ne abundance higher by only a factor of 2.5^{5,6}—quite within our estimated range.

Extensive review articles on the coronae of the Sun and stars document evidence that coronal chemical compositions often appear different to those thought to characterise the underlying photospheres.^{9,16–18} The differences appear to relate to element first ionisation potentials (FIPs): the solar corona appears enhanced in elements with low FIP (≤ 10 eV; e.g., Mg, Si Fe),^{9,16} whereas much more coronally active stars appear to have depletions in low FIP elements and perhaps enrichments of high FIP elements (≤ 10 eV; e.g., O, Ne, Ar).^{16–18} At first sight, this chemical fractionation might render direct interpretation of coronal abundance ratios in terms of the composition of the underlying star problematic. However, that we are seeing the same Ne/O ratio in a wide variety of stars sampling a large range of different coronal activity levels indicates that there is no significant fractionation between O and Ne in disk-integrated light from stellar coronae. This leads us to conclude that the results represent the true Ne/O abundance ratios of these stars. This conclusion is bolstered by findings of a constant Ne/O abundance ratio, in good agreement with our value, for a small sample of single and active binary stars observed by *XMM-Newton*.^{18,19} In view of the consistency of the Ne/O abundance ratio in nearby stars, it seems likely that the solar ratio should be similar.

There are no recent full-disk integrated light Ne/O measurements for the Sun; existing studies are instead based on observations of particular regions and structures of the solar outer atmosphere. We provide a tabular summary and bibliography of some of the different Ne/O estimates since 1974

as Supplementary Information to this letter. While the preponderance of estimates appear consistent with current assessments, the underlying observations do not sample photospheric material. The Ne/O ratio is in fact observed to differ substantially between the different observations. In particular, the highest measured Ne/O ratios based on X-ray lines are 2-3 times the accepted solar value and are compatible with the abundance ratio we find for nearby stars. These higher Ne/O ratios were obtained for hotter active regions^{13,20} that are likely to dominate the solar full-disk X-ray emission. These measurements are the most directly compatible with the ones presented here based on full-disk integrated light X-ray spectra of stars.

Similarly “high” Ne/O ratios have also been seen in γ -ray observations of flares, ³He-rich solar energetic particle events, and in the decay phase of long duration soft X-ray events.²¹⁻²³ The γ -ray measurements probe material that is irradiated by downward-flowing accelerated particles.^{21,22} The particle beams penetrate through to the chromosphere which is likely more representative of the underlying photospheric material than coronal regions.

Recent sophisticated models of heliospheric pickup ion and anomalous cosmic ray populations from the local interstellar medium are also inconsistent with the current solar Ne/O abundance ratio, but could be reconciled by raising this to $A_{Ne}/A_O \sim 0.53$,²⁴ which is similar to our values for nearby stars. This Ne/O ratio is somewhat higher than the mean from studies of ionized nebulae in the Milky Way and other galaxies, but falls within the scatter of results at solar metallicity.²⁵

The implication of our study, then, is that the higher of the observed solar Ne/O abundance ratios are the ones representative of the underlying solar composition. This scenario is in accordance with our observations of Ne/O in nearby stars and reconciles solar models with helioseismology.

Methods

We use the resonance lines of H-like O and of H-like and He-like Ne to estimate the Ne/O abundance ratio. In hot (10^6 - 10^7 K) coronal plasma these lines are formed predominantly by radiative

de-excitation of levels excited by collisions with thermal electrons. The flux, F_{ji} , from such a transition $j \rightarrow i$ in an ion of an element with abundance A can be written as

$$F_{ji} = A \int_{\Delta T_{ji}} G_{ji}(T) \Phi(T) dT \text{ erg cm}^{-2} \text{ s}^{-1} \quad (1)$$

where $G_{ji}(T)$ describes the line *emissivity*—the product of the relative population of the ion in question and the excitation rate of the transition as a function temperature, T . The kernel $\Phi(T)$ —the emission measure distribution—describes the excitation power of the plasma as a function of temperature, which is proportional to the mean of the square of the electron density, N_e , and the emitting volume V , $\Phi(T) = \overline{N_e^2}(T) \frac{dV(T)}{dT}$.

If we can choose O and Ne lines whose $G_{ji}(T)$ functions have very similar temperature dependence, an abundance ratio by number, A_{Ne}/A_O , can be derived simply from the ratio of their observed line fluxes, F_O and F_{Ne} , since all the temperature-dependent terms in Equation 1 cancel:

$$\frac{A_{Ne}}{A_O} = \left(\frac{G_O}{G_{Ne}} \right) \frac{F_{Ne}}{F_O} \quad (2)$$

An early study of Ne/O ratios in solar active regions¹³ used the ratio of Ne IX $1s2p^1P_1 \rightarrow 1s^2^1S_0$ to O VIII $2p^2P_{3/2,1/2} \rightarrow 1s^2S_{1/2}$. This ratio does, however, have some significant residual dependence on temperature.¹³ Here we remove much of this temperature dependence by addition of Ne X $2p^2P_{3/2,1/2} \rightarrow 1s^2S_{1/2}$; our combined Ne $G_{ji}(T)$ function is $G_{Ne} = G_{NeIX} + 0.15G_{NeX}$. The resulting ratio G_O/G_{Ne} is illustrated as a function of temperature in Figure 3. We have verified the small residual temperature sensitivity evident in the lower panel of Figure 3 to be negligible for our analysis by integrating the products of G_O and G_{Ne} with empirically-derived emission measure distributions, $\Phi(T)$, for different stars,^{12,26} and for functions $\Phi \propto T^a$, with $1 \leq a \leq 4$: the integrated emissivity ratio from these tests was $\int \Phi G_O dT / \int \Phi G_{Ne} dT = 1.2 \pm 0.1$. We conclude that the line ratio method is robust and the higher Ne/O abundance ratio found here will not be significantly changed through performing full emission measure distribution modelling.

We measured Ne and O line fluxes (listed in Table 1) from *Chandra* HETG X-ray spectra obtained directly from the Chandra public data archive (<http://cda.harvard.edu>). Final listed fluxes

for Ne X include small reductions ($\leq 15\%$ for 17 out of 21 of our stars, and 25-37% for the remainder) to account for a weak blend of Fe XVII at 12.12 Å. The Fe XVII 12.12 Å contribution was estimated by scaling the observed strengths of unblended Fe XVII lines at 15.26, 16.77, 17.05 and 17.09 Å (the strong 15.01 Å resonance line was omitted to avoid potential problems with its depletion through resonance scattering) by their theoretical line strengths relative to the 12.12 Å line as predicted by the CHIANTI database. Minor blending in the wings of the Ne IX 13.447 Å line was accounted for by fitting simultaneously with the neighbouring weaker lines, comprised of a Fe XIX-XXI blend at 13.424 Å and Fe XIX 13.465 Å, following a detailed study of these features in the Capella binary system.²⁷ Since these blend corrections are generally very small, the uncertainties in these procedures have negligible ($< 10\%$) influence on the derived Ne/O abundance ratios.

1. Bahcall, J. N., Basu, S., Pinsonneault, M. & Serenelli, A. M. Helioseismological Implications of Recent Solar Abundance Determinations. *Astrophys. J.* **618**, 1049–1056 (2005).
2. Asplund, M., Grevesse, N. & Sauval, J. The solar chemical composition. *ArXiv Astrophysics e-prints astro-ph/0410214* (2004). astro-ph/0410214.
3. Basu, S. & Antia, H. M. Constraining Solar Abundances Using Helioseismology. *Astrophys. J. Lett.* **606**, L85–L88 (2004).
4. Bahcall, J. N., Serenelli, A. M. & Basu, S. New Solar Opacities, Abundances, Helioseismology, and Neutrino Fluxes. *Astrophys. J. Lett.* **621**, L85–L88 (2005).
5. Antia, H. M. & Basu, S. The Discrepancy between Solar Abundances and Helioseismology. *Astrophys. J. Lett.* **620**, L129–L132 (2005).
6. Bahcall, J. N., Basu, S. & Serenelli, A. M. What Is The Neon Abundance Of The Sun? *ArXiv Astrophysics e-prints astro-ph/0502563* (2005). astro-ph/0502563.
7. Bahcall, J. N., Serenelli, A. M. & Pinsonneault, M. How Accurately Can We Calculate the Depth of the Solar Convective Zone? *Astrophys. J.* **614**, 464–471 (2004).

8. Asplund, M., Nordlund, Å., Trampedach, R. & Stein, R. F. Line formation in solar granulation. II. The photospheric Fe abundance. *Astron. Astrophys.* **359**, 743–754 (2000).
9. Meyer, J.-P. The baseline composition of solar energetic particles. *Astrophys. J. Suppl. Ser.* **57**, 151–171 (1985).
10. Anders, E. & Grevesse, N. Abundances of the elements - Meteoritic and solar. *Geochim. Cosmochim. Acta.* **53**, 197–214 (1989).
11. Grevesse, N. & Sauval, A. J. Standard Solar Composition. *Space Science Reviews* **85**, 161–174 (1998).
12. Drake, J. J. *et al.* Enhanced Noble Gases in the Coronae of Active Stars. *Astrophys. J. Lett.* **548**, L81–L85 (2001).
13. Acton, L. W., Catura, R. C. & Joki, E. G. Oxygen-to-neon abundance ratio in the solar corona. *Astrophys. J. Lett.* **195**, L93–L95 (1975).
14. Canizares, C. R. *et al.* High-Resolution X-Ray Spectra of Capella: Initial Results from the Chandra High-Energy Transmission Grating Spectrometer. *Astrophys. J. Lett.* **539**, L41–L44 (2000).
15. Sanz-Forcada, J., Favata, F. & Micela, G. Coronal versus photospheric abundances of stars with different activity levels. *Astron. Astrophys.* **416**, 281–290 (2004).
16. Feldman, U. & Laming, J. M. Element Abundances in the Upper Atmospheres of the Sun and Stars: Update of Observational Results. *Phys. Scripta* **61**, 222–252 (2000).
17. Drake, J. J. Chemical fractionation and abundances in coronal plasma. *Advances in Space Research* **32**, 945–954 (2003).
18. Güdel, M. X-ray astronomy of stellar coronae. *Astron. Astrophys. Rev.* **12**, 71–237 (2004).
19. Audard, M., Güdel, M., Sres, A., Raassen, A. J. J. & Mewe, R. A study of coronal abundances in RS CVn binaries%. *Astron. Astrophys.* **398**, 1137–1149 (2003).

20. Schmelz, J. T., Saba, J. L. R., Ghosh, D. & Strong, K. T. Anomalous Coronal Neon Abundances in Quiescent Solar Active Regions. *Astrophys. J.* **473**, 519–532 (1996).
21. Murphy, R. J., Ramaty, R., Reames, D. V. & Kozlovsky, B. Solar abundances from gamma-ray spectroscopy - Comparisons with energetic particle, photospheric, and coronal abundances. *Astrophys. J.* **371**, 793–803 (1991).
22. Ramaty, R., Mandzhavidze, N., Kozlovsky, B. & Murphy, R. J. Solar Atmospheric Abundances and Energy Content in Flare Accelerated Ions from Gamma-Ray Spectroscopy. *Astrophys. J. Lett.* **455**, L193–L196 (1995).
23. Schmelz, J. T. Elemental abundances of flaring solar plasma - Enhanced neon and sulfur. *Astrophys. J.* **408**, 373–381 (1993).
24. Frisch, P. C. & Slavin, J. D. The Chemical Composition and Gas-to-Dust Mass Ratio of Nearby Interstellar Matter. *Astrophys. J.* **594**, 844–858 (2003).
25. Henry, R. B. C. & Worthey, G. The Distribution of Heavy Elements in Spiral and Elliptical Galaxies. *Publ. Astron. Soc. Pac.* **111**, 919–945 (1999).
26. Garcia-Alvarez, D. *et al.* The FIP effect on late-type stellar coronae: from dwarfs to giants. *AAS/High Energy Astrophysics Division* **8**, 10.03 (2004).
27. Ness, J., Brickhouse, N. S., Drake, J. J. & Huenemoerder, D. P. Modeling the Ne IX Triplet Spectral Region of Capella with the Chandra and XMM-Newton Gratings. *Astrophys. J.* **598**, 1277–1289 (2003).
28. Kashyap, V. & Drake, J. J. PINTofALE : Package for the interactive analysis of line emission. *Bulletin of the Astronomical Society of India* **28**, 475–476 (2000).
29. Mazzotta, P., Mazzitelli, G., Colafrancesco, S. & Vittorio, N. Ionization balance for optically thin plasmas: Rate coefficients for all atoms and ions of the elements H to NI. *Astron. Astrophys. Suppl.* **133**, 403–409 (1998).

30. Young, P. R. *et al.* CHIANTI-An Atomic Database for Emission Lines. VI. Proton Rates and Other Improvements. *Astrophys. J. Suppl. Ser.* **144**, 135–152 (2003).

Supplementary Information Supplementary Information accompanies this paper on www.nature.com/nature

Acknowledgements JJD was supported by a NASA contract to the *Chandra X-ray Center*. PT was supported by a Chandra award issued by Chandra X-ray Center, which is operated by SAO for and on behalf of NASA. JJD thanks the NASA AISRP for providing financial assistance for the development of the PINTOfALE package. We thank Drs. G. Share, R. Murphy, W. Ball and D.Garcia-Alvarez for useful discussions and comments.

Competing interests statement The authors declare that they have no competing financial interests.

Correspondence Correspondence and requests for materials should be addressed to J.J. Drake (email: jdrake@cfa.harvard.edu).

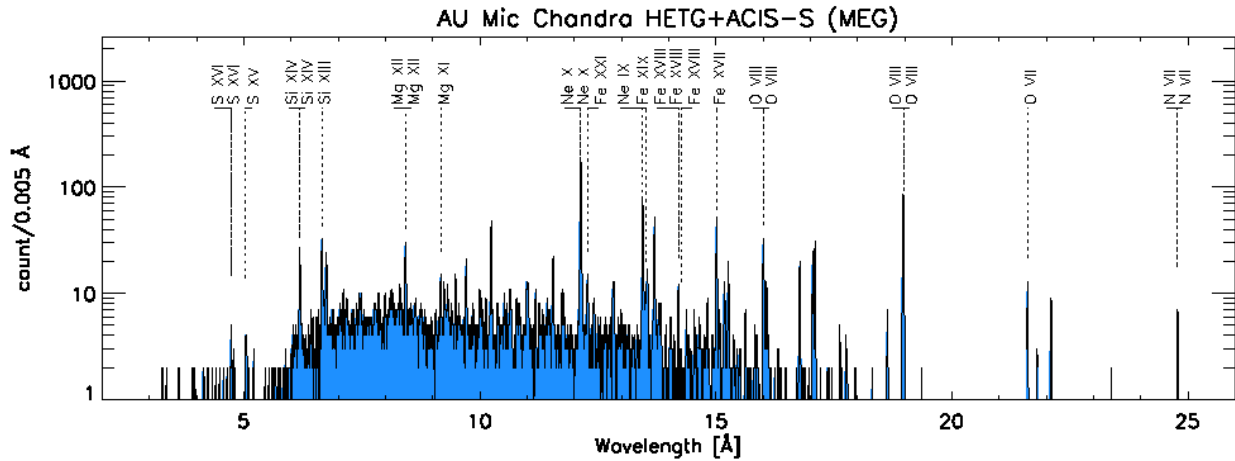


Figure 1: A *Chandra* Medium Energy Grating X-ray spectrum of the M1 V star AU Mic. These data are typical of the *Chandra* MEG spectra upon which this study is based. Emission line features superimposed on the bremsstrahlung continuum are formed predominantly by radiative decay of transitions excited by electron impact. Prominent lines are labelled, including the lines of O VIII $2p^2P_{3/2,1/2} \rightarrow 1s^2S_{1/2}$ (18.97 Å), Ne IX $1s2p^1P_1 \rightarrow 1s^2^1S_0$ (13.45 Å) and Ne X $2p^2P_{3/2,1/2} \rightarrow 1s^2S_{1/2}$ (12.13 Å) used here to determine the Ne/O abundance ratio.

Table 1: Spectral line fluxes and derived Ne/O abundance ratios for the stars analysed in this study. Line fluxes were measured from the Medium Energy Grating (MEG) component of *Chandra* HETG spectra by line profile fitting using the Package for Interactive Analysis of Line Emission (PINTofALE) software²⁸ (freely available from <http://hea-www.harvard.edu/PINTofALE>). The effective collecting area of the instrument was accounted for using standard *Chandra* calibration products and techniques (see <http://cxc.harvard.edu/ciao/> for details). Ne/O abundance ratios were obtained assuming the O/Ne line emissivity ratio of $\int \Phi G_O dT / \int \Phi G_{Ne} dT = 1.2 \pm 0.1$, as described in Methods. Stated flux and abundance ratio uncertainties correspond to 1σ limits.

| Star | Type | Dist. [pc] | log (L_X/L_{bol}) | Line Fluxes (10^{-13} erg cm $^{-2}$ s $^{-1}$) | | | |
|---------------|--------------|---------------|--------------------------|---|-----------------|-----------------|-----------------|
| | | | | F_{NeIX} | F_{NeX} | F_{OVIII} | A_{Ne}/A_O |
| AU Mic | M1V | 9.9 | -3.37 | 3.08 ± 0.20 | 5.60 ± 0.24 | 10.4 ± 0.4 | 0.38 ± 0.05 |
| Prox Cen | M5Ve | 1.3 | -3.92 | 0.70 ± 0.14 | 1.22 ± 0.4 | 3.2 ± 0.3 | 0.28 ± 0.22 |
| EV Lac | M1.5V | 5.1 | -3.11 | 3.09 ± 0.10 | 3.99 ± 1.0 | 9.16 ± 0.20 | 0.40 ± 0.19 |
| AB Dor | K0V | 15 | -3.26 | 4.9 ± 0.4 | 10.7 ± 0.4 | 14.6 ± 0.5 | 0.44 ± 0.06 |
| HR9024 | G1III | 135 | -3.65 | 0.30 ± 0.11 | 2.09 ± 0.18 | 2.40 ± 0.23 | 0.26 ± 0.15 |
| 31 Com | G0III | 94 | -4.70 | 0.21 ± 0.05 | 0.84 ± 0.08 | 1.30 ± 0.17 | 0.27 ± 0.13 |
| β Cet | K0III | 29.4 | -5.35 | 2.15 ± 0.09 | 5.30 ± 0.14 | 8.0 ± 0.3 | 0.37 ± 0.04 |
| Canopus | F0II | 96 | -7.23 | 0.52 ± 0.10 | 0.76 ± 0.05 | 1.33 ± 0.25 | 0.48 ± 0.15 |
| μ Vel | G5III/... | 35.5 | -5.46 | 1.40 ± 0.13 | 1.80 ± 0.24 | 4.2 ± 0.3 | 0.40 ± 0.11 |
| Algol | B8V/K1IV | 28 | -3.5 | 2.9 ± 0.3 | 12.8 ± 0.7 | 13.8 ± 0.5 | 0.35 ± 0.09 |
| ER Vul | G0V/G5V | 50 | -3.45 | 1.10 ± 0.11 | 3.0 ± 0.19 | 3.8 ± 0.3 | 0.41 ± 0.10 |
| 44 Boo | G1V/G2V | 13 | -4.16 | 3.75 ± 0.29 | 8.1 ± 0.4 | 15.2 ± 0.6 | 0.33 ± 0.06 |
| TZ CrB | G0V/G0V | 22 | -3.36 | 7.63 ± 0.30 | 15.5 ± 0.4 | 22.1 ± 0.5 | 0.45 ± 0.04 |
| UX Ari | G5V/K0IV | 50 | -3.63 | 3.62 ± 0.27 | 12.4 ± 0.3 | 9.7 ± 0.5 | 0.56 ± 0.08 |
| ξ UMa | G0V/G0V | 7.7 | -4.26 | 4.56 ± 0.24 | 5.41 ± 0.22 | 15.8 ± 0.6 | 0.34 ± 0.03 |
| II Peg | K2V/... | 42 | -2.92 | 5.26 ± 0.30 | 19.4 ± 0.5 | 19.4 ± 0.8 | 0.42 ± 0.06 |
| λ And | G8III/... | 26 | -4.53 | 2.79 ± 0.20 | 8.82 ± 0.23 | 10.3 ± 0.4 | 0.40 ± 0.05 |
| TY Pyx | G5IV/G5IV | 56 | -3.55 | 2.09 ± 0.22 | 4.78 ± 0.09 | 4.9 ± 0.5 | 0.57 ± 0.08 |
| AR Lac | G2IV/K0IV | 42 | -3.72 | 2.7 ± 0.3 | 9.70 ± 0.28 | 9.3 ± 0.5 | 0.45 ± 0.07 |
| HR1099 | G5IV/K1IV | 29 | -3.29 | 8.36 ± 0.26 | 27.6 ± 0.3 | 27.9 ± 0.5 | 0.45 ± 0.03 |
| IM Peg | K2III-II/... | 97 | -3.98 | 3.00 ± 0.29 | 15.8 ± 0.3 | 13.0 ± 0.7 | 0.41 ± 0.06 |

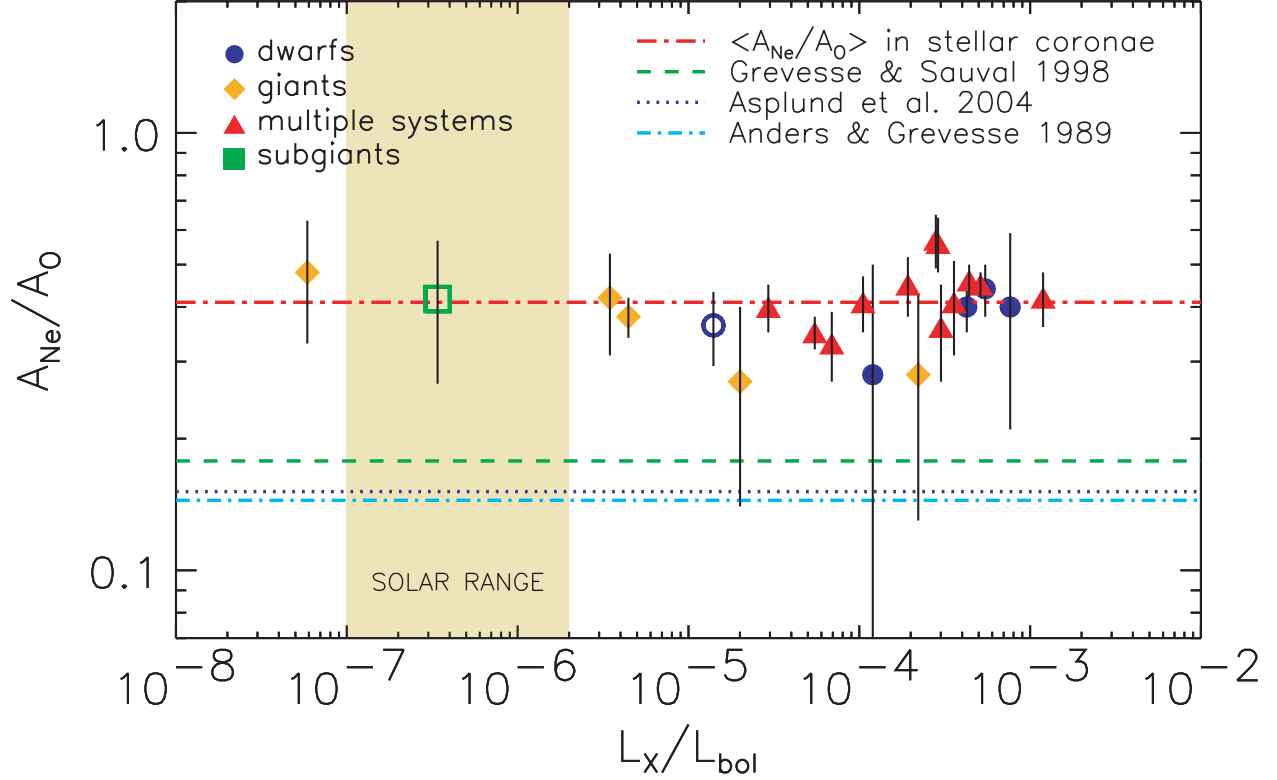


Figure 2: Derived Ne/O abundance ratios by number, A_{Ne}/A_O , vs. the coronal activity index L_X/L_{bol} . Error bars represent quadrature addition of 1σ uncertainties of line flux measurement. Also shown using hollow symbols are literature values¹⁵ for the stars Procyon (F5 IV) and ϵ Eri (K2 V) observed using the *Chandra* Low Energy Transmission Grating Spectrometer (LETGS) to better represent the lower ranges of coronal activity. The error-weighted mean Ne/O abundance ratio is $A_{Ne}/A_O = 0.41$, or 2.7 times the currently assessed value² which is illustrated by the dashed horizontal line. The recommended value from comprehensive earlier assessments in common usage^{10,11} are also illustrated.

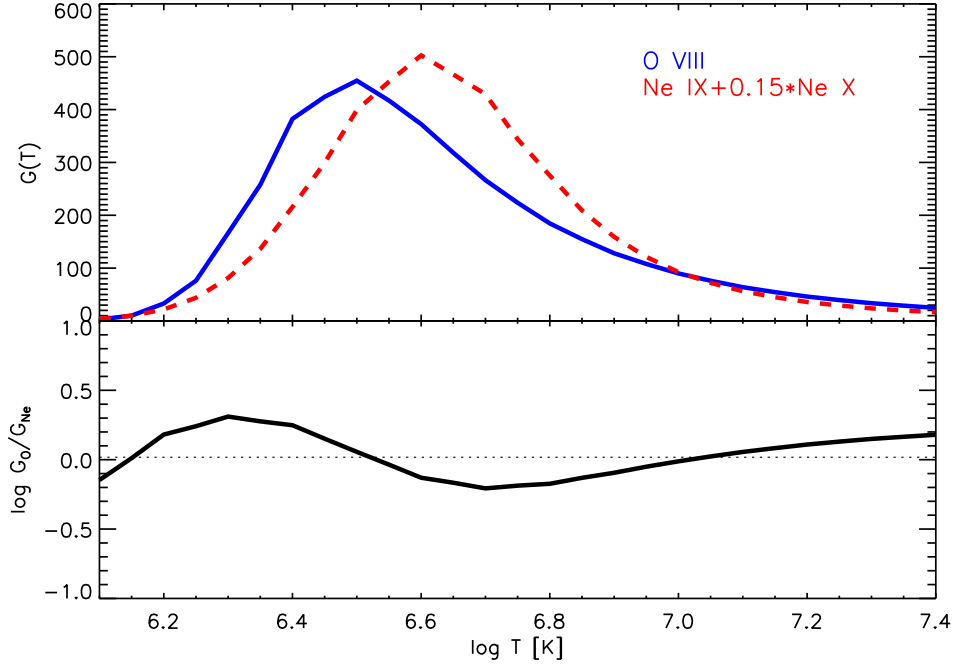


Figure 3: The temperature-insensitive O/Ne emissivity ratio. The upper panel illustrates the emissivities G_O , of the O VIII $2p^2P_{3/2,1/2} \rightarrow 1s^2S_{1/2}$ line, and G_{Ne} of the Ne IX $1s2p^1P_1 \rightarrow 1s^2^1S_0$ and Ne X $2p^2P_{3/2,1/2} \rightarrow 1s^2S_{1/2}$ lines combined as $G_{Ne} = G_{NeIX} + 0.15G_{NeX}$. The lower panel shows the logarithmic ratio G_O/G_{Ne} . Emissivities are based on electron excitation rates and ion populations²⁹ compiled in the CHIANTI database,³⁰ as implemented in PINTofALE.²⁸